Journal Homepage: -www.journalijar.com

INTERNATIONAL JOURNAL OF ADVANCED RESEARCH (IJAR)

Article DOI:10.21474/IJAR01/24570
DOI URL: http://dx.doi.org/10.21474/IJAR01/24570

RESEARCH ARTICLE

RECONCILING ENERGY, COMFORT, COST AND CARBON IN A TROPICAL DWELLING: A MANY-OBJECTIVE STUDY FOR BENIN

Bome Brice [1], Fannou Jean-Louis Comlan[2], Tokpohozin Noukpo Bernard[2] and Houngan Comlan Aristide [3]

1. Laboratory of Engineering Sciences and Applied Mathematics (LSIMA) of the National University of Sciences, Technologies Engineering and Mathematics of Abomey (UNSTIM-Abomey), Benin.
2. Associate Professor, Laboratory of Engineering Sciences and Applied Mathematics (LSIMA) of the National University of Sciences, Technologies Engineering and Mathematics of Abomey (UNSTIM-Abomey), Benin.
3. Full Professor, Laboratory of Engineering Sciences and Applied Mathematics (LSIMA) of the National University of Sciences, Technologies Engineering and Mathematics of Abomey (UNSTIM-Abomey), Benin.

Manuscript Info

Manuscript History
Received: 12 September 2026
Final Accepted: 14 October 2026
Published: November 2026

Key words:-
multi-objective optimization; adaptive metamodel; NSGA-III; ceiling fan; mixed adaptive comfort; raw earth; tropical climate; Energy Plus.

Abstract

Designing a house in a tropical climate requires reconciling often conflicting criteria: reducing electricity consumption, ensuring thermal comfort, optimizing costs, minimizing the carbon footprint of materials, and maintaining habitability during power outages.This study optimizes sixteen design options according to these five objectives. Each configuration is evaluated through two full annual simulations using Energy Plus.Since simulations are costly, to limit their number, a surrogate model, built from previously performed simulations, guides NSGA-III toward new configurations, which are then simulated and added to the model training set. Twenty independent searches led to 5,994 simulated configurations. The 972 selected configurations were fully re-simulated, with an average difference between estimated and simulated values of less than 4.3% for each of the five objectives. Among these, 445 are not dominated by any configuration in the overall set, and 412 are validated by a second dominance analysis. All 445 configurations feature earthen walls, with no concrete or conventio nal block walls, and this structure remains unchanged even when the price and carbon footprint of the materials vary by ± 20%. The ceiling fan, whose energy consumption and heat dissipation are included in the calculation, accounts for a median of 16.9% of total electricity consum ption, rising to as much as 83.3%. Its benefit lies in the ability to raise the air conditioning setpoint.

"© 2026 by the Author(s). Published by IJAR under CC BY 4.0. Unrestricted use allowed with credit to the author."

Introduction:-

Designing buildings in hot and humid tropical climates, such as the one in Bohicon, Benin, presents a major challenge: reconciling energy consumption, thermal comfort, and economic viability. In this context, air conditioning represents a significant portion of energy consumption, with high operating costs and substantial environmental impacts. The demand for cooling in sub-Saharan Africa is growing faster than the electrical grids designed to meet it.

Corresponding Author:- Bome Brice
Address:-Laboratory of Engineering Sciences and Applied Mathematics (LSIMA) of the National University of Sciences, Technologies Engineering and Mathematics of Abomey (UNSTIM-Abomey), Benin.

Integrating this need into basic domestic demand increases the required electrification investments by approximately two-thirds [1], and the saturation of existing air conditioning systems is following a trajectory already documented in comparable climates [2, 3]. Design decisions made today therefore have implications that extend beyond occupant comfort.

Three recurring limitations characterize bioclimatic optimization in tropical climates. The first concerns the operation of ceiling fans, whose electrical consumption and heat dissipated in the room are rarely included in the same energy balance [4, 5, 6, 7]. The second concerns thermal comfort. Field studies conducted in Benin, Nigeria, and other comparable tropical regions show neutral temperatures and adaptation margins that differ from assumptions based on temperate climates [8, 9, 10, 11, 12, 13, 14, 15, 16, 17]. The third limitation concerns the optimization methodology itself. Most bioclimatic optimization studies vary four to seven building envelope parameters under two or three objectives. A limited computational budget often prevents verification of the stability of the compromise when the initialization of the search change. A single stochastic search therefore does not allow us to clearly distinguish the structure of the problem from the effect of the initial draw [18, 19, 20, 21, 22, 23, 24, 25].

This study extends an earlier study devoted to the energy balance of mixing in the same building, entitled " Multi-objective optimization of the energy performance of a BIM model of a residential building Accepted for publication in the journal *International Journal on Emerging Technologies* (ISSN No. (P): 0975-8364, (O): 2249-3255). This initial work explored 11 variables and 3 objectives through direct optimization. The present study extends the design space to 16 variables and 5 objectives, uses a surrogate model to limit the number of full simulations, and repeats the search twenty times before re-evaluating the building configurations selected in EnergyPlus. The problem addressed, the search strategy, and the validation protocol are therefore different from the initial work. These three questions are addressed within a single framework. The fan is integrated into the room's thermal balance. Comfort is calculated hour by hour according to the room's actual conditions. The building envelope and energy regulation are jointly optimized across sixteen variables and five objectives, and then the selected building designs are verified through comprehensive simulation.

Materials and Methods:-

Materials:-

Building and climate environment:-

The building studied is described in Table 1. The geometric model comes from a BIM export to EnergyPlus [32, 33]. The original wall assemblies, made of lightweight panels, were reconstructed as variable load-bearing walls in order to represent earth materials and their inertia.

Table 1. Building and simulation characteristics.

Element	Description
Location	Bohicon, Benin, 7.18°N and 2.07°E
Building	Residential patio house on two levels, 221 m2 ^{of} living space
Zoning	35 thermal zones, including 17 air-conditioned and 19 inhabited
Envelope	521 m² ^{of} exterior walls
Meteorology	TMYx weather dataset from OneBuilding [34], file BEN_ZO_Bohicon.653380_TMYx.epw

The meteorological file corresponds to a typical meteorological year. No external wet-bulb temperature approximation is introduced [35].

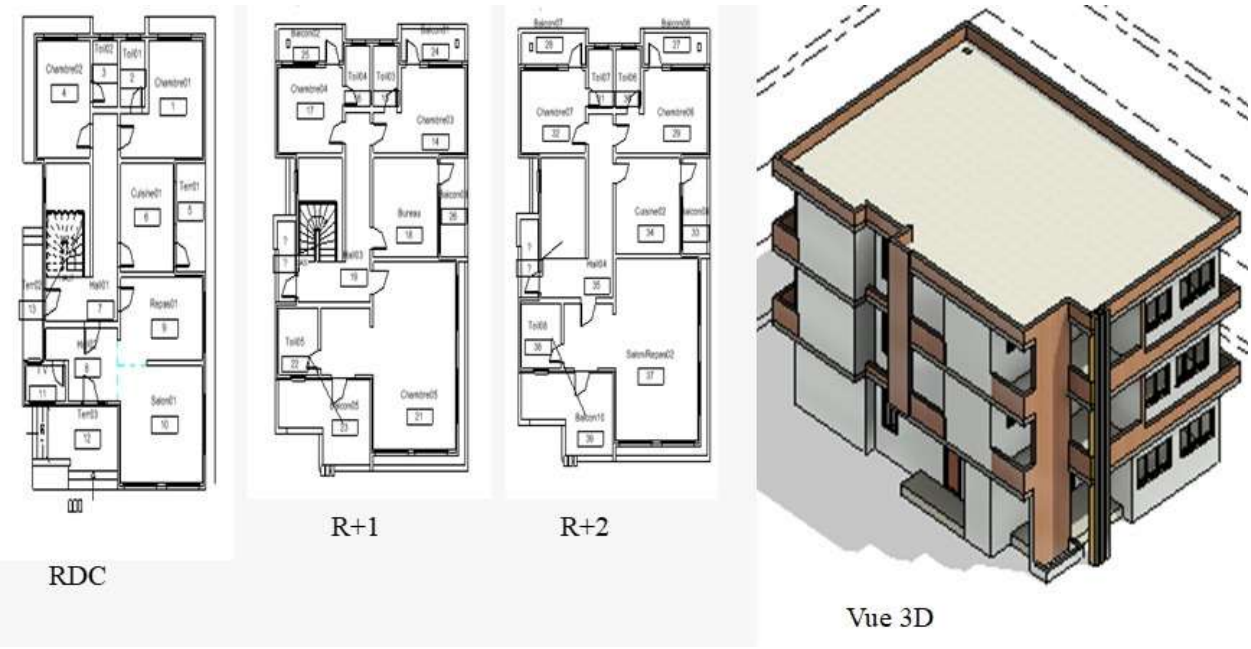

Architectural plans and 3D view of the building model under study

Simulation tools and computing environment:-

The main tools used to build the model, perform energy simulations and carry out optimization are summarized in Table 2. The versions are kept fixed throughout the calculations so that successive evaluations remain comparable.

Table 2. Simulation, calculation and optimization tools.

Tool	Version	Function in the study
EnergyPlus [33]	25.2	Annual energy simulation of the building and production of hourly outputs.
Python	3.10	Exepower outageion environment for data processing, optimization and adjustment of numerical surrogate models.
NumPy	2.2.6	Numerical calculation and manipulation of data tables.
SciPy	1.15.3	Scientific computing, statistics and complementary numerical operations.
scikit-learn	1.7.2	Adjustment and validation of learning models used as numerical surrogate models.
Pymoo	0.6.1.6	Implementation of multi-objective optimization , including NSGA-III.
Logging	JSONL	Recording of evaluations, design variables and results to ensure traceability of successive enrichments.

This chain separates the energy assessments carried out by EnergyPlus from the numerical processing performed in Python and ensures the traceability of successive calculations.

Methods:-

Operating strategy:-

The building's operating mode consists of a cooling strategy organized according to three levels: natural ventilation, mechanical air movement by fans, and then air conditioning.

It is imposed by two temperature thresholds, relative to the monthly adaptive neutral temperature [36, 37]:-

$$T_{fan} = \min\left(T_n + \Delta T_f, T_{max} - \delta\right), T_{clim} = \min(T_{fan} + \Delta T_s, T_{max}), \quad (1)$$

With $T_{max} = 29°C$ and a hierarchy margin $\delta = 0{,}5K$, which guarantees that a fan remains operable under the air conditioning setpoint regardless of the draw of ΔT_f and ΔT_s.

Physical and energy models:-

Thermal comfort and the effect of air movement:-

Thermal comfort is modeled according to the Fanger model defined by ISO 7730 [38]. The PMV is written:

$$\mathrm{PMV}=\left(0{,}303e^{-0{,}036\,M}+0{,}028\right)L,[38,\,39] \quad (2)$$

where is the metabolic rate and thermal load of the body, a function of the clothing surface temperature , unique solution of [38]:MLt_{cl}

$$t_{cl}=t_{sk}-I_{cl}\left[3{,}96\times10^{-8}f_{cl}\left((t_{cl}+273)^4-(t_r+273)^4\right)+f_{cl}\,h_c(t_{cl}-t_a)\right], \quad (3)$$

This equation is solved by a Newton method secured by bounding (the strict monotonicity of the residue guarantees the uniqueness of the root).

The predicted percentage of dissatisfied occupants is [38]:

$$\mathrm{PPD}=100-95\exp\left(-0{,}03353\mathrm{PMV}^4-0{,}2179\mathrm{PMV}^2\right). \quad (4)$$

The building is neither fully air-conditioned nor entirely free-running: depending on the design, between 13% and 76% of occupied hours are actually air-conditioned, with the remainder provided by natural ventilation and mechanical air movement. Thermal comfort is therefore assessed hourly, zone by zone, according to the actual simulated conditions.

$$\mathrm{PMV}_{\mathrm{eff}}(t)=\begin{cases}\mathrm{PMV}(t) & \text{climatisation active à l'instant t,}\\ e_{\mathrm{adapt}}\mathrm{PMV}(t) & \text{régime libre à l'instant t,}\end{cases} \quad e_{\mathrm{adapt}}=0{,}9, \quad (5)$$

in the spirit of extending PMV to non-air-conditioned buildings in hot climates [40], transposed to West African field surveys [8, 9]. The objective, f_2i.e. thermal comfort, aggregates this effective PMV, weighted by occupancy and surface area, over inhabited areas Z_h:

$$f_2=\frac{1}{S_h}\sum_{z\in Z_h}A_z\,\frac{\sum_t n_{occ}\,(z,t)\mathrm{PPD}\,(z,t)}{\sum_t n_{occ}\,(z,t)},\ S_h=\sum_{z\in Z_h}A_z. \quad (6)$$

Beyond 0.2 m s^{-1} , the PMV of ISO 7730 falls outside its range of validity; however, the fan increases the air velocity to 1.2 m s^{-1} at its highest setting. The normative correction of ASHRAE 55-2023 [41, 42, 43], based on Gagge's two-node model [44], brings the calculation back within its range: the temperature reduction called Cooling Effect , denoted CE, is calculated. At 0.1 m s^{-1}, this produces the same standard effective temperature as the actual ventilated environment. The PMV is then evaluated . Three thermal comfort treatments were compared using the same set of simulations. The first uses Fanger alone, the second applies the expectancy factor in both regimes, and the third corresponds to the selected mixed formulation. No significant reversal of dominance results; only the magnitude of the comfort gain depends on the treatment.$(t_a\text{-CE},\,t_r\text{-CE},\,0.1\mathrm{m/s})$

Air circulation: flow rate, speed and power:-

The fan is an electrical device whose heat is included in the zone's energy balance. The heat loss is zero, as nothing leaves the room, and it is controlled by a temperature sensor specific to each equipped zone. The air velocity it induces follows the measured model of Raftery et al. [31, 5], fitted to 78 chamber tests:

$$s_o=0{,}99\frac{D}{R}-0{,}06\frac{H_{\mathrm{pale}}}{D}+0{,}11\frac{D}{H_{\mathrm{occ}}}+0{,}274,\ R=\sqrt{A_z}, \quad (7)$$

$$S_F=\frac{4(Q/60)}{\pi D^2},\ v_{\mathrm{fan}}=\min(s_o S_F,\,2.76\mathrm{m/s}), \quad (8)$$

Or is the fan diameter, the blade installation height, m the height of the occupied zone, and the nominal flow rate. The 2.76 m s −1 limit is that of the domain on which the correlation was adjusted. It never encroaches on this building: the maximum reached is 2.275 m s −1 . The air speed used credited to the comfort calculation remains capped at 1.2 m s −1 , in accordance with ASHRAE 55 §5.3.3.1, which mandates local control by the occupant [41]. This condition allows the air conditioning setpoint to be raised in the presence of air movement. The power and flow rate follow the selected speed setting :$DH_{\mathrm{pale}}\,H_{\mathrm{occ}}=1{,}7Qx_{17}$

$$P(f)=P_{\max}f^{1,32},\ Q(f)=Q_{\max}f, \quad (9)$$

The exponent 1.32 is adjusted to the power ratios measured at the three notches of an induction motor. The local product provides 30.0 W/120 m 3 min −1 at the low-speed setting, 51.3 W/180 m 3 min −1 at the medium-speed setting and 75.0 W/240 m 3 min −1 at the high-speed setting.

Infiltration and energy consumption:-

The air conditioner is not an ideal system with a constant coefficient of performance: its degradation under partial load is modeled by the default correlation of EnergyPlus [33, 45] for a single-stage direct expansion coil ,

$$PLR_z(t)=\frac{\dot{Q}_{froid,z}(t)}{\dot{Q}_{cap,z}},\ PLF_z(t)=0{,}85+0{,}15PLR_z(t), \quad (10)$$

Hence the need for cooling electricity and the objective f_1:

$$E_{clim}=\sum_z\sum_t\frac{\dot{Q}_{froid,z}(t)}{COP\cdot PLF_z(t)},\ f_1=E_{clim}+E_{fan},\ COP=2{,}6. \quad (11)$$

Infiltration follows the surface of the exterior wall, standardization of ASHRAE Fundamentals ch. 16 [46], and not the glazing/floor ratio erroneously used in an earlier version of the model:

$$ACH_z=\begin{cases}k\frac{A_{ext,z}}{V_z} & A_{ext,z}>0,\\ 0.10/h & A_{ext,z}=0,\end{cases} \quad (12)$$

The coefficient kbeing set once for all the building so that the volume-weighted average is worth 0.278/h, the only literature level value of the infiltration model (not measured locally, see Discussion section).

Optimization problem:-

Design variables and constraints:-

Sixteen design variables describe the building envelope, shading, natural ventilation, mechanical air movement, and air conditioning control. These are presented in Table 3. Air conditioning capacity is not included: it is automatically sized by EnergyPlus over the design days, with a safety factor of 1.15, in accordance with ASHRAE sizing practice [47], to avoid ever undersizing an unfavorable combination. The number of ceiling fans is an integer rather than a continuous surface power: expressing air movement as continuous would place the optimum on equipment that is not commercially available.3.

Table 3. Design variables, domains and origin of the bounds.

Variable	Kind	Domain	Basis for the bounds
x_1 SHGC glazing	Continuous	[0.20; 0.70]	local catalogue of glazing, from single clear glazing to solar control film glazing [48]
air-conditioning setpoint offset x_2	Continuous	[0.5; 3.0] K	Hierarchy margin between fan and air conditioning, with δ=0,5K
number of ceiling fans x_4	Discrete	{0,…,19}	number of habitable rooms that can actually be equipped, depending on the building's geometry
fan speed setting x_{17}	Categorical	{low, medium, high}	notches of the locally marketed product, in 56 inches
x_5 fan threshold	Continuous	[0; 3] K	deviation from adaptive neutral temperature [36]
x_6 azimuth	continuous, circular	[0 ; 360]°	building orientation
x_7 opening fraction VN	Continuous	[0.05; 0.40]	the actually openable portion of a standard bay
x_8 VN opening threshold	Continuous	[22; 26] °C	minimum nighttime value of the local weather file
x_9 VN triggering deviation	Continuous	[0.5; 3.0] K	usual maintenance differential
x_{10} wall material	categorical, 4	n / A .	catalogue of materials presented in table 4
x_{11} wall thickness	normalized continuous	[0 ; 1]	mapped onto [,] of the material , calibrated on the daytime thermal penetration depth $e_{min}\ e_{max}\ x_{10}\ \delta=\sqrt{\alpha\cdot 24h/\pi}$
x_{12} roof insulation	categorical, 5	n / A .	catalogue of materials presented in table 5
x_{13} insulation thickness	normalized continuous	[0 ; 1]	mapped onto [,] of the insulation according to ISO 10456 [49] $e_{min}\ e_{max}\ x_{12}$
x_{14} roof overhang	Continuous	[0.05; 0.90] window height×	lower bound imposed by EnergyPlus (non-zero shading area)

Variable	Kind	Domain	Basis for the bounds
x_{15} roof reflectance	Continuous	[0.15; 0.85]	range of available roofing materials (from dark matte to cool-roof)
x_{16} VN draw height	Continuous	[1.0; 3.5] m	stack height, geometric range ground floor/upper floor

Two categorical variables refer to a catalogue of materials located in West Africa, whose properties and sources are listed in Tables 4 and 5. The indices are treated as categorical and never interpolated: a stationary core interpolated between concrete and adobe would produce a material that does not exist.

Table 4. Wall materials from the catalogue for x_{10}.

Material	λ[W /(m K)]	ρ[kg/ m³]	GWP [kgCO_2 eq/kg]	lifetime	Source
Concrete (concrete block)	1.40	2200	0.13	50 years	ISO 10456, generic concrete
BTC, cement 6%	0.95	1950	0.045	40 years	BTC literature West Africa [21]
Adobe (raw earth)	0.58	1550	0.010	25 years	raw earth literature, high variability [21]
Compacted laterite	1.15	2000	0.015	35 years	Regional literature, local resource (Zou)

Table 5. Roof insulation from the catalogue for x_{12}.

Insulation material	λ[W /(m K)]	ρ[kg/ m³]	GWP [kgCO_2 eq/kg]	Source
imported reference PUR foam	0.026	35	3.40	industrial data sheets, ICE database
Rock wool	0.040	80	1.05	general mineral wool data sheets
Typha fiber	0.050	200	0.06	typha literature Sahel/Senegal
Rice husk	0.062	120	0.015	literature on agricultural residues [50]
Palm kernel fiber	0.075	140	0.010	to be characterized locally (placeholder)

The fan selected as the commercial reference is an induction model with a diameter of 1.42 m, a nominal flow rate of 240 m^3 / min , and a nominal power of 75 W. These specifications are taken from the manufacturer's datasheet used for the Cotonou market. Three speed settings are derived from the same physical power model described in the section " Air Circulation: Flow Rate, Speed, and Power" .

Objective functions:-

The vector of objectives, all to be minimized, is summarized in Table 6. The attempts at objective reduction are interpreted with the relative delta error of Brockhoff and Zitzler [51] and the ε-dominance [25].6.

Table 6. Objective vector, all to be minimized.

	Size	Unit	Operating condition
f_1	Annual electricity consumption (cooling + fans)	kWh	air-conditioned
f_2	Discomfort, dissatisfied occupants	%	air-conditioned
f_3	Discounted construction and maintenance cost	FCFA	:
f_{4a}	Embodied carbon of materials	kgCO_2 eq	:
f_{5c}	Overheating degree-hours without air conditioning	Kh·	power outage

Each is governed by a distinct family of variables: energy and comfort by active thermal regulation (, ,), cost and carbon by envelope materials associated with variables at , and resistance to power outages by natural ventilation ( ). This separation is measured, not assumed: a target removal test (Brockhoff and Zitzler relative deviation) places all

five above the redundancy threshold, and removing them one by one would change between 28% and 63% of the recommended design decisions.$x_2x_4x_5x_{10}x_{13}x_9$

Operational carbon is calculated as the product of electricity and the network emission factor. The discounted bill is calculated and reported, but excluded from the optimization vector: these are increasing affine transformations f_1(ρSpearman's ratio = 1.000 measured), which would not provide any additional decision-making power. The cost $f_3$includes investment items related to glazing, walls and insulation, air conditioners, fans, awnings) and maintenance and replacements discounted over a 20-year horizon, at an actual rate of 3% per year:

$$f_3=C_{invest}+\sum_{cycles\ d'entretien}\frac{C_{cycle}}{(1+\tau)^n}+\sum_{remplacements}\frac{C_{remp}}{(1+\tau)^n},\ \tau=0{,}03. \quad (13)$$

The term maintenance and replacement, based on the lifespan of the material and not its energy performance, is what makes it $f_3$independent of f_1: an adobe wall is the cheapest to install and the most expensive to maintain. The embodied carbon f_{4a}relates only to the building envelope materials [52, 53] (×GWP mass, including transport, replacements over the study period); the refrigerant carbon, which follows the installed capacity and not the material, is calculated and reported separately and is not included in the optimization. It is constant to within 0.6%, with the smallest unit on the market (1,758 kW) exceeding the load of each room in this building.

Resistance to outages $f_{5c}$is measured on a separate simulation, with air conditioning disabled, in degree-hours of overheating above 30°C, weighted by occupancy and surface area:

$$f_{5c}=\frac{1}{S_h}\sum_{z\in Z_h}A_z\sum_t\max\left(t_a(z,t)-30{,}0\right)n_{occ}(z,t). \quad (14)$$

Depending only on a temperature balance, this variant is structurally more robust than a variant based on the PPD in free-running conditions, whose calculation would pass through the air velocity in natural ventilation, which constitutes the least assured link in the model.

Optimization strategy:-

Each configuration requires approximately 660 seconds of computation (two annual simulations, air-conditioned and free-running): exhaustively scanning sixteen variables is impractical. The search proceeds in two stages (Figure 1).

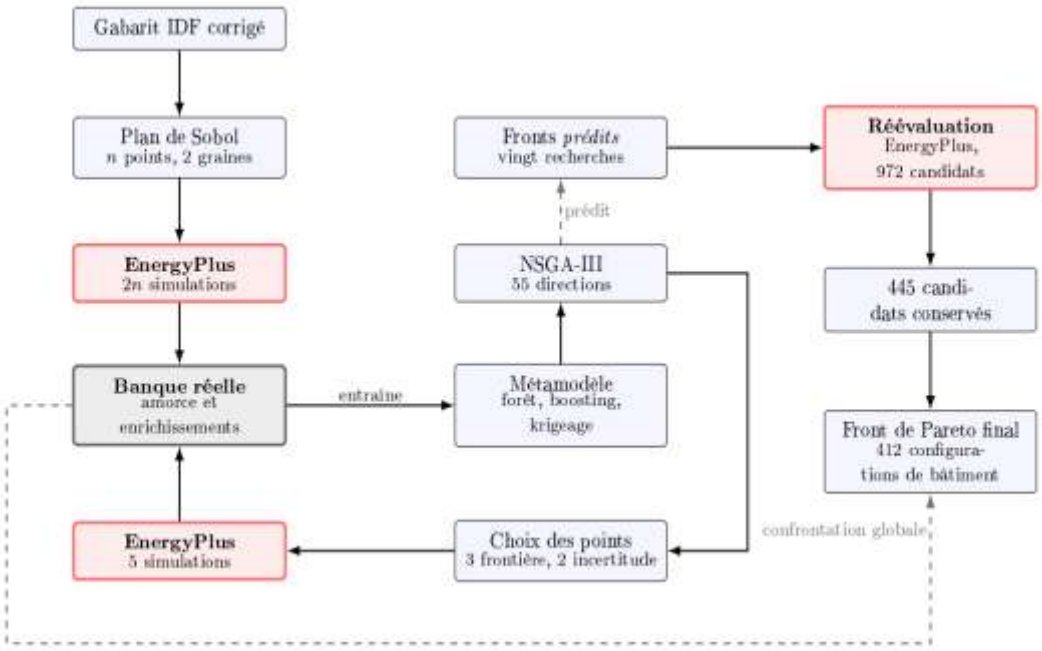

Figure 1. Search guided by surrogate model, then re-evaluation in EnergyPlus

Figure 1 distinguishes the database of full EnergyPlus simulations from the evaluations performed on the rapid numerical model. The new building configurations selected during the research are then re-evaluated in EnergyPlus, thus separating the research phase from the verification phase.1

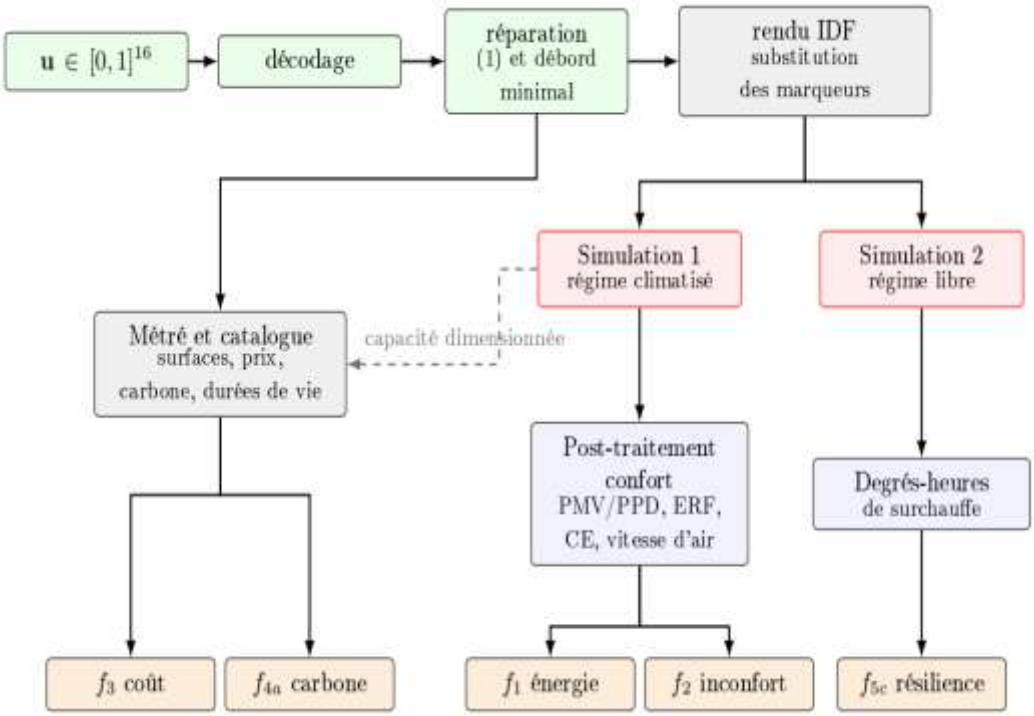

Figure 2. Evaluation chain of an individual. Two annual simulations feed into the objectives derived from thehourly series; the cost $f_3$and carbon $f_{4a}$are recalculated a posteriori from the logged data.

Figure 2 details the calculation of a building configuration. The two annual simulations provide energy, comfort, and resilience indicators, while the quantity survey and catalogue data allow for the calculation of cost and embodied carbon without rerunning EnergyPlus. NSGA-III [24, 23] uses the reference directions of Das and Dennis [54]. For mobjectives and pdivisions, their number is

$$H=\binom{m+p-1}{p}. \quad (15)$$

The chosen protocol uses 55 directions and 100 internal generations for each optimization of the surrogate model.
An initial set of 512 building configurations is constructed using a Sobol sequence. This is a quasi-random, low-discrepancy design that evenly distributes points in the design space [55, 56]. Owen scrambling is applied to this sequence. Two independent designs each serve as primers for ten searches. They use distinct scrambles and share no points. This choice allows the effect of initial sampling to be distinguished from that of the stochastic search. A hypercube Latin design would have a different extension structure [57].

The surrogate model, based on kriging or gradient boosting depending on the objective, is selected through five-fold cross-validation. It predicts the five objectives and provides an uncertainty estimate based on a a common kriging model. In each cycle, five building configurations are simulated in EnergyPlus: three close to the Pareto front and two chosen based on aggregate uncertainty. Near duplicates are discarded before this selection. The predicted values are never reintroduced into the simulation database.

We refer to this model-assisted search as SAEA. In each cycle, the surrogate model is refitted using all building configurations simulated to date, and then NSGA-III explores the approximated space. Five new building configurations are selected for full simulation: three near the Pareto front and two in regions where model uncertainty is highest. Only these configurations are replenished with the simulation database. The search terminates when the hypervolume [58] of the simulation database no longer grows for five cycles, under a session budget of 11.5 hours.

The computing chain uses EnergyPlus 25.2 and Python 3.10. The main libraries are numpy 2.2.6, scipy 1.15.3, scikit-learn 1.7.2, and pymoo 0.6.1.6. The material catalog fingerprint is recorded in each log line so that a data change explicitly invalidates previous logs. Searches are distributed across multiple remote computing sessions, each writing a resumable log.

Final check:-

A compromise produced by a surrogate model remains a hypothesis until it is confirmed by the full simulator. For each search, the final predicted front, obtained after refitting the metamodel to the complete database and then rerunning NSGA-III, is fully re-simulated. The 972 building configurations from the twenty searches were thus resimulated in EnergyPlus, without any failures. This re-evaluation then constitutes an inter-search validation step: 445 candidates are not dominated by any of the 5994 configurations in the overall database, and a second dominance analysis among these candidates reduces the validated Pareto front to 412 building configurations.

To formalize this distinction, we have V_{972} the set of candidates from the twenty terminal fronts actually verified, and B_{5994} the bank of all simulated configurations. Denoting f(x) the vector of the five objectives, all minimized, the retained candidates are

$$S_{445}=\{x \in V_{972} : \nexists y \in B_{5994} \text{ tel que } f(y) \preccurlyeq f(x), f(y) \neq f(x)\}, \quad (16)$$

where denotes component-by-component dominance. The same non-dominance operator is then applied to $\preccurlyeq$

$$P_{412}=ND(S_{445}), |S_{445}|=445, |P_{412}|=412. \quad (17)$$

Results:-

From research to the Pareto front validated:-

The twenty searches, spread across the two initial samples, total 5994 truly simulated and distinct configurations (the 512 starting points, common to the ten searches for the same plan, are counted only once). Mud walls occupy 100% of the best building configuration found, across both samples and without exception. Compared to its own research, each verified building configuration remains optimal in 85.5% of cases on average. Compared to all 5994 configurations produced by the twenty combined research studies, this more demanding comparison lowers this rate to 45.8% , leaving 445 candidates retained after overall validation. This decrease reflects the benefit of pooling twenty independent searches rather than just one: each retained building configuration withstood comparison with nineteen additional studies. Among these 445 retained candidates, 33 are subsequently outperformed by another retained candidate; the final validated Pareto front therefore comprises 412 building configurations . The 445 retained candidates consume between 1419 and 11325 kWh per year, with a dissatisfaction rate of 13.5%–26.4%.

Figure 3 shows the transition from the 972 re-evaluated building configurations to the subset of 445 retained configurations, and then to the final front.

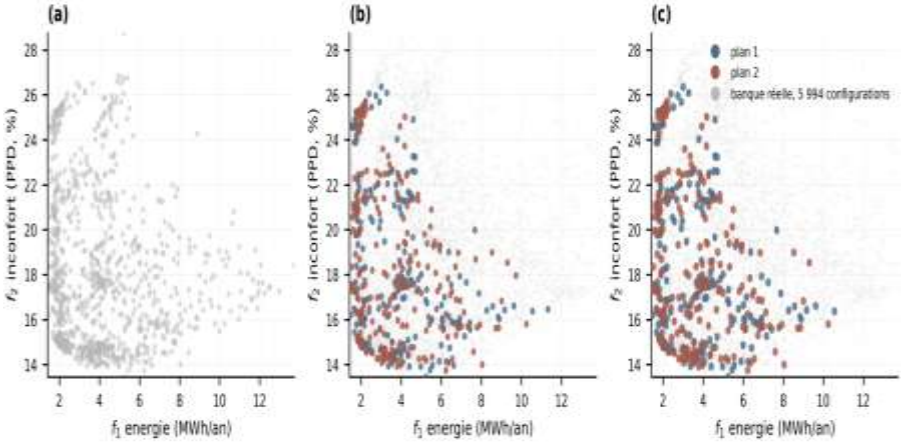

Figure 3. Validation of building configurations and final Pareto front

Figure 3 summarizes the validation of building performance. Figure 3a shows the 972 configurations re-evaluated in EnergyPlus. Figure 3b retains the 445 configurations that are not dominated by any of the 5,994 configurations in the overall database across the five criteria studied. These the retained solutions represent more favorable energy–comfort trade-offs. The scatter plot concentrates downwards and to the left, forming a set of higher-performing solutions. Figure 3c then removes the 33 configurations that are still dominated by each other, leading to a final Pareto front comprising 412 building configurations. This will allow a designer to choose the precise building configuration depending on whether the best balance between energy performance and occupant thermal comfort is sought. The 445 configurations thus constitute the set retained after validation, while 412 form the final Pareto compromise.3

Metamodel reliability and validation:-

Table 7 compares, for each of the five objectives, the value predicted by the metamodel to the value actually simulated, for the 972 verified configurations.7

Table 7. Prediction/simulation discrepancies on the 972 verified configurations.

Objective	Mean relative error	inter-search standard deviation	maximum error	Signed bias	NRMSE
f_1 energy	4.29%	0.87%	33.22%	-0.77%	0.0183
f_2 discomfort	2.01%	0.25%	14.19%	-0.22%	0.0341
f_3 cost	0.25%	0.05%	1.79%	0.04%	0.0030
f_{4a} carbon	0.37%	0.08%	4.41%	-0.07%	0.0020
f_{5c} resilience	1.92%	0.30%	15.60%	-0.20%	0.0105

Bias is more important for interpretation than the mean error alone: a centered error cancels out between compared building configurations, while a bias shifts the front as a whole. Here, all biases remain below 0.77%, slightly optimistic except for the cost. The inter-search standard deviation, much lower than the mean error, shows that this error is a property of the metamodel and not of any particular search. Figure 4 presents the comparison between the predictions of the fast numerical model and the results of EnergyPlus.

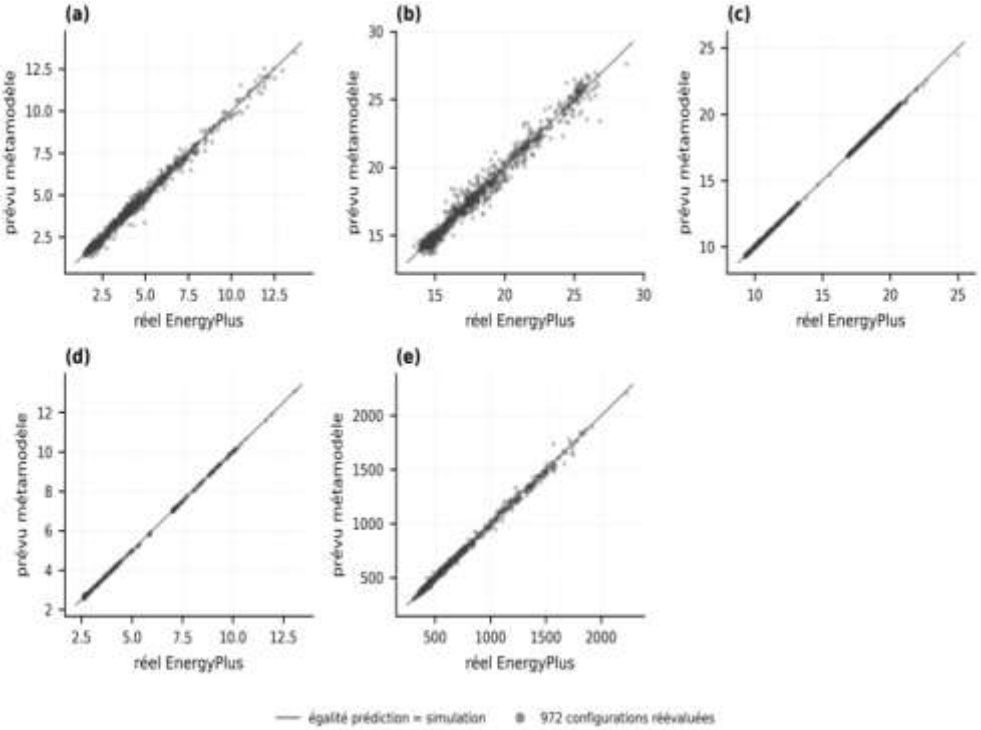

Figure 4. Predicted values and simulated values.

Figure 4 compares the metamodel predictions with the EnergyPlus results for the five building performance criteria (Figures 4a–4e). The data points lie close to the 1:1 line. Annual energy use exhibits the largest mean prediction error, while the other objectives show smaller discrepancies.4 7.

Interactions between objectives and variables:-

A sensitivity analysis based on the Shapley effects of the metamodel [59, 60, 61] attributes to each variable its share of responsibility in each of the five objectives. Three families of levers govern the five objectives, without overlapping: the pilot fan activation threshold accounts for 42.7% of the annual energy variation, ahead of the air conditioning setpoint temperature (19.8%); the number of ceiling fans controls 54.1% of the discomfort; the wall material controls 65.3% of the cost and 87.9% of the embodied carbon; the natural ventilation opening threshold controls 58.8% of the resistance to power outages.

This separation leads to an important result: construction costs are independent of energy consumption, as different variables govern them, but they are at odds with embodied carbon, with the wall material influencing both simultaneously in opposite directions. Laterite is cheap and carbon-intensive; adobe is more expensive but less carbon-intensive. Therefore, none of the five objectives can be deduced from the others. Figure 5 shows the relative importance of the variables for each of the five objectives.

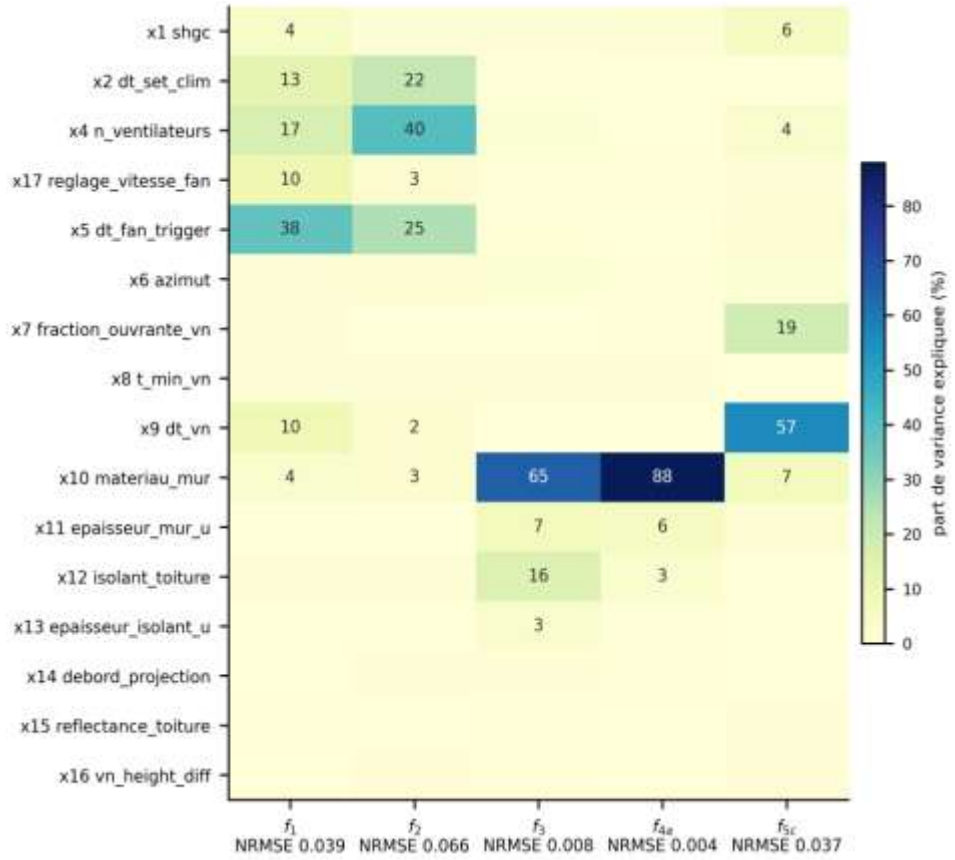

Figure 5. Relative importance of design variables on performance objectives assessed by Shapley effects

Figure 5 links design variables to the mechanisms that determine building performance. The fan activation threshold accounts for 42.7% of the annual energy variation, followed by the air conditioning setpoint at 19.8%. The number of ceiling fans accounts for 54.1% of the variation in discomfort. The wall material contributes to 65.3% of the cost variation and 87.9% of the embodied carbon variation. For periods without air conditioning, the natural ventilation opening threshold accounts for 58.8% of the resilience variation. The figure thus allows us to identify the physical levers associated with each criterion. Figure 6 shows the direction and strength of the monotonic associations between the ordered variables and the objectives.5 6

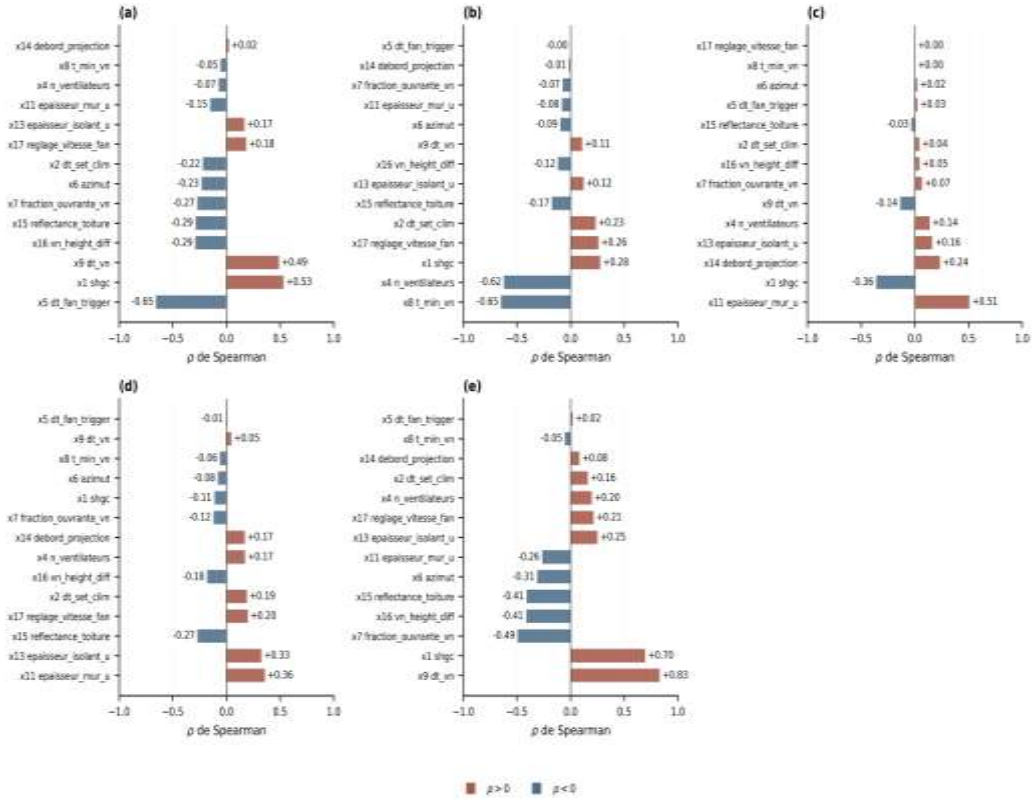

Figure 6. Spearman correlations between variables and objectives

Figure 6 clarifies the direction of the observed relationships between design variables and building performance. Panels (a) through (e) represent energy, discomfort, cost, embodied carbon, and resilience, respectively. Material categorical variables are not artificially ordered and are therefore not shown. The coefficients thus indicate which design modifications are associated with an increase or decrease in each criterion. The figure complements Shapley's analysis, which primarily provides information on the relative importance of the variables.

Materials, carbon and sensitivity:-

From a material standpoint, the convergence is clear: of the 972 building configurations verified, none of the walls are made of concrete or cement-stabilized compressed earth blocks shown in Table 8. The two types of raw earth, adobe and laterite, account for almost equal proportions of all the building configurations verified in both initial samples. The subset of 445 candidates retained after validation also remains entirely composed of raw earth.

Table 8. Composition of the 972 verified building configurations.

Wall	**Part**	**Insulation material**	**Part**
Adobe (raw earth)	51.2%	Palm kernel fiber	86.0%
Compacted laterite	48.8%	Typha fiber	4.8%
Concrete, BTC cement	0%	Rice husk	4.2%
		Rock wool	3.3%
		PUR Foam	1.6%

The cost and carbon footprint analysis of the selected building designs reveals a clear separation between two groups, based on wall material: laterite occupies the most economical branch but has the highest carbon footprint, while adobe is more expensive and is the only material at the lower end of the carbon spectrum. The cost and carbon trade-off therefore occurs within the raw earth construction itself, not between raw earth and concrete. Figure 7 shows the composition of the envelopes, their cost-carbon trade-off and sensitivity to the catalogue assumptions.

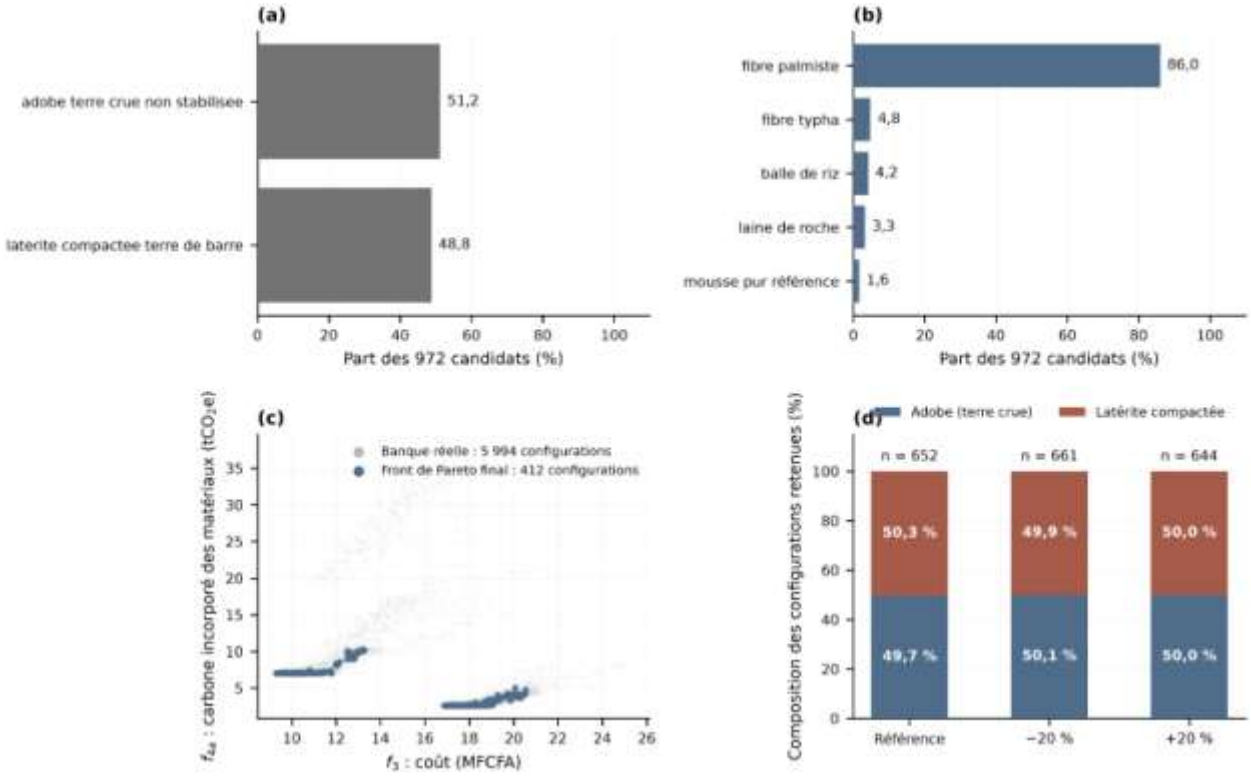

Figure 7. Material structure of the trade-offs and sensitivity to price and emission assumptions.

Figure 7 presents, in Figure 7a, the composition of the walls, in Figure 7b, that of the insulation, and in Figure 7c, the trade-off between cost and embodied carbon. Adobe and laterite walls represent 51.2% and 48.8%, respectively, of the 972 verified configurations. Palm kernel fiber represents 86.0% of the insulation. Figure 7c positions the 412 final front configurations relative to the 5,994 configurations of the simulation database on the cost and carbon axes.
Panel (d) shows that the composition between adobe and laterite varies by a few tenths of a point when prices and emission factors vary by 20%. The material trend therefore remains stable despite these catalog uncertainties.7 Material prices and emission factors remain estimates. The 972 verified building configurations were re-evaluated under two perturbed catalogs (costs and emissions multiplied uniformly by 0.80 and then by 1.20), without new simulations. Neither energy consumption nor comfort depends on material prices. Table 9 compares the composition of the best building configuration under the three hypotheses.

Table 9. Composition of the best-performing configuration under perturbed material costs and embodied-carbon factors.±20%

	Reference	-20%	+20%
Selected configurations	652	661	644
Adobe part	49.7%	50.1%	50.0%
Laterite part	50.3%	49.9%	50.0%

The distribution between the two raw earths only changes by a few tenths of a point, and concrete remains absent under the three scenarios: the conclusion does not depend on the prices retained. Of the 972 building configurations examined, the median construction cost is lower than that of a conventional concrete block design: 8.33 million CFA francs compared to 14.49 million CFA francs. The discounted electricity bill over twenty years is also lower: 7.92 million CFA francs compared to 15.01 million CFA francs. Over twenty years, the median total cost is 23.21 million CFA francs compared to 30.07 million CFA francs. The difference lies in the cost structure: earthen walls replace some of the capital investment with maintenance costs, which are absent with concrete blocks, and the electricity savings close the gap.

This comparison, however, must be interpreted with two caveats. The maintenance of earthen walls remains a theoretical assumption, not a field measurement, and it is precisely the fan that determines the comparison. The two

populations overlap: only 37.3% of the building configurations in the compromise fall below the best observed concrete block. The defensible argument, therefore, is that raw earth shifts the cost distribution, not that it systematically dominates concrete blocks.

Figure 8 shows the structure and distribution of cumulative expenditure over twenty years.

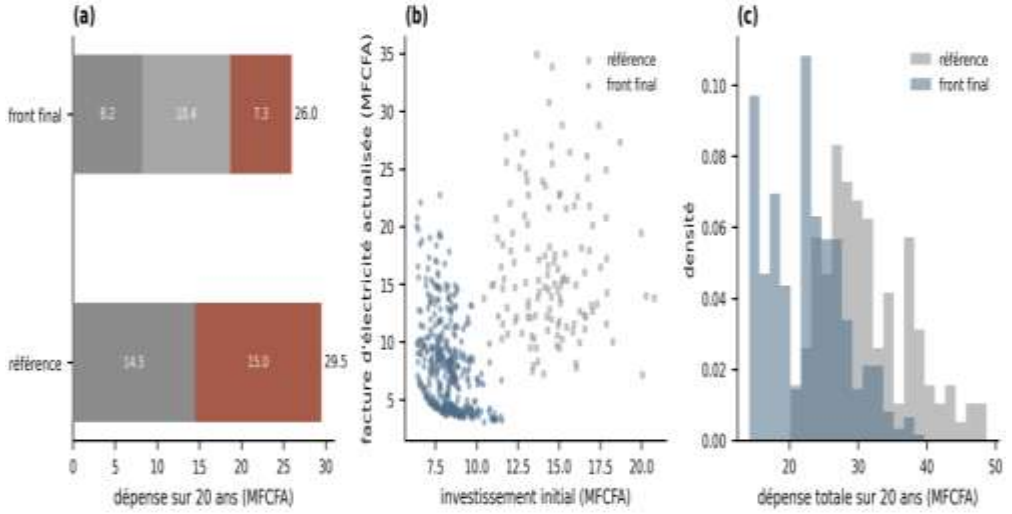

Figure 8. Expenditure over twenty years

Figure 8 breaks down the expenditure over twenty years. Figure 8a distinguishes between construction, maintenance, and electricity. Figure 8b links the initial investment to the discounted electricity bill for the reference concrete block and the final frontage. Figure 8c shows the recovery of total expenditures. The medians of the 972 verified configurations remain at 8.33 million CFA francs compared to 14.49 million CFA francs for construction, 7.92 million CFA francs compared to 15.01 million CFA francs for the discounted bill, and 23.21 million CFA francs compared to 30.07 million CFA francs for the total expenditure over twenty years. The observed savings therefore stem from both the initial investment and electricity consumption over the analysis period.

Energy efficiency and operating costs:-

Air circulation is generally presented as a negligible expense. Measured across the 5,994 simulated configurations, this item represents a median of 16.9% of total electricity consumption, and up to 83.3%; more than half of the configurations exceed 10%. Accounting that ignores this item, and the heat the motor transfers to the room, would overestimate the net benefit of air movement.

Figure 9 shows the role of mixing in consumption, comfort, cooling effect and partial load operation.

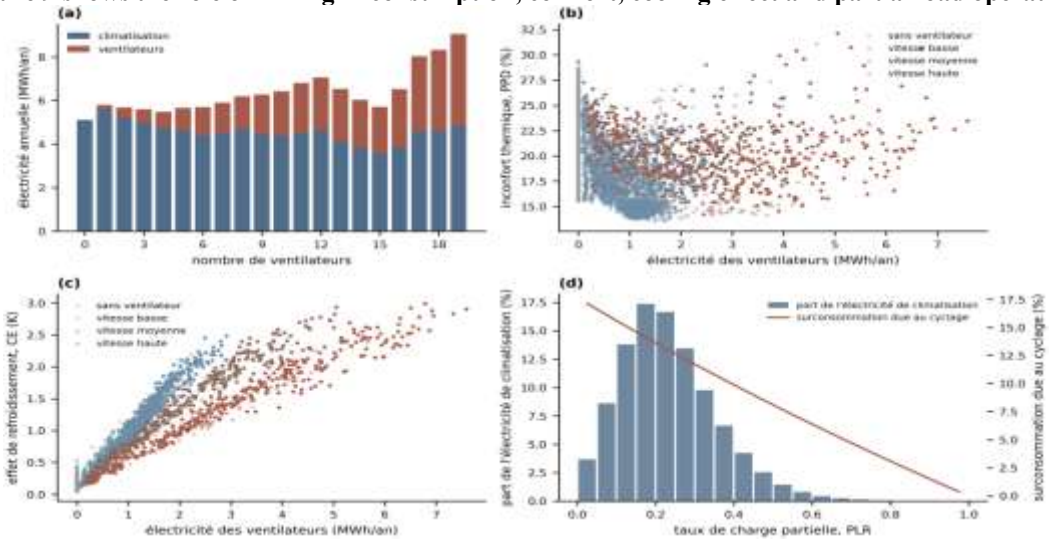

Figure 9. Energy performance

Figure 9 details the energy consumption of air movement and air conditioning. Figure 9a shows the respective contributions of air conditioning and fans as the number of units increases. Figure 9b links the electricity consumed by fans to thermal discomfort and distinguishes between the three fan speeds and the absence of fans. Figure 9c links this consumption to the cooling effect (CE). Figure 9d shows the distribution of air conditioning electricity according to the partial load factor and the overconsumption associated with cycling. Across the 5,994 configurations, fans account for a median of 16.9% of the total electricity consumption, rising to as high as 83.3%, thus justifying their inclusion in the energy balance.9 9a 9b 9c 9d

Robustness, convergence and reproducibility:-

The reproducibility between the twenty searches can also be quantified: the average distance between two final compromises, out of the one hundred and ninety possible pairs, remains less than the inherent precision of each compromise taken in isolation. The disagreement between searches is smaller than the resolution at which a single search already describes the compromise surface. Table 10 compares the same error between the two initial samples: across the five objectives, the difference between plans remains less than the dispersion within the same plan; the initial draw does not determine the result.

Table 10. Intra-plane dispersion versus inter-plane deviation (mean relative error).

Objective	Plan 1	Plan 2	Difference
f_1	4.18 % ± 0,66	4.41 % ± 1,02	0,23 pt
f_2	2.00 % ± 0,18	2.03 % ± 0,31	0,03 pt
f_3	0.26 % ± 0,06	0.24 % ± 0,03	0,02 pt
f_{4a}	0.38 % ± 0,09	0.36 % ± 0,06	0,02 pt
f_{5c}	1.94 % ± 0,34	1.90 % ± 0,26	0,04 pt

Figure 10 shows the evolution of the optimization process across cycles.10

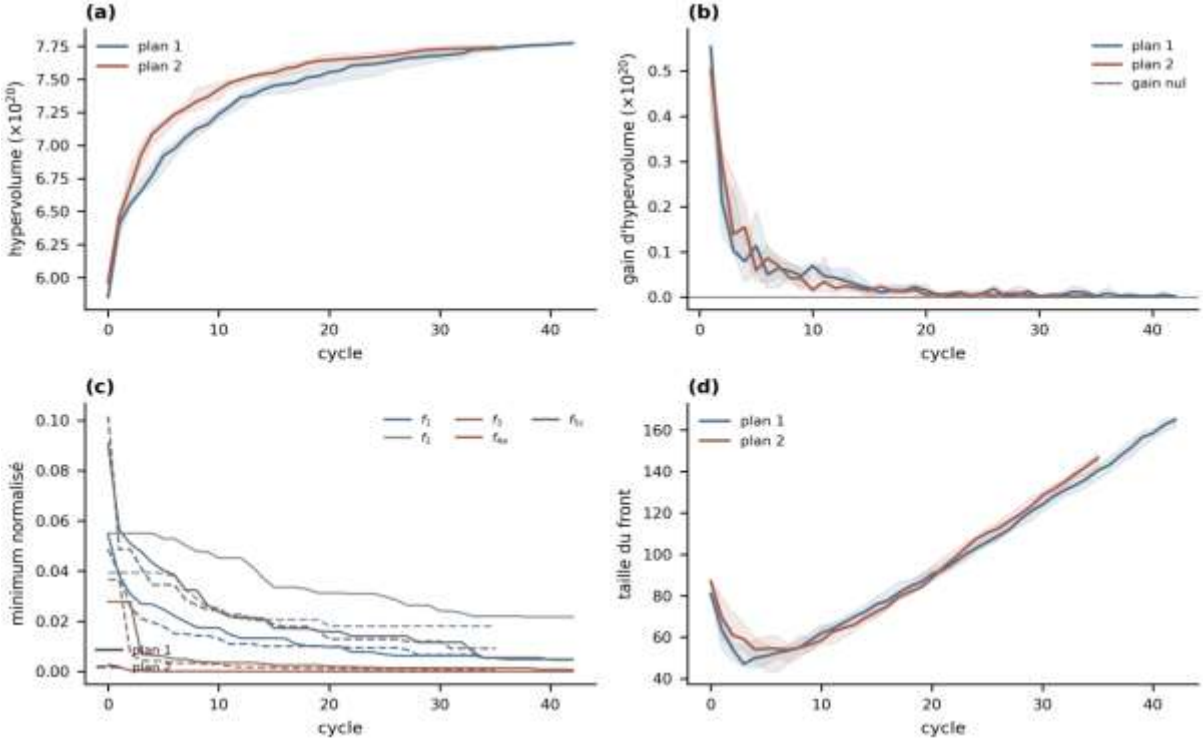

Figure 10. Convergence

Figure 10 presents four complementary indicators of the performance progression. Figure 10a tracks the evolution of the hypervolume of the simulation database for the two initial plans. Figure 10b shows the gain obtained from one cycle to the next. Figure 9c tracks the normalized minima of the five criteria and verifies that the improvement does not stem from a single aspect of building performance. Figure 9d shows the evolution of the number of non-dominated configurations. The simultaneous stabilization of these indicators marks the attainment of a regime where new simulations bring few improvements to the energy, thermal, economic, and environmental trade-offs.10 9a 9b 9c 9d 10 9a 9b 9c 9d

Figure 11 shows the dispersion between the twenty searches and between the two initial sampling plans.11

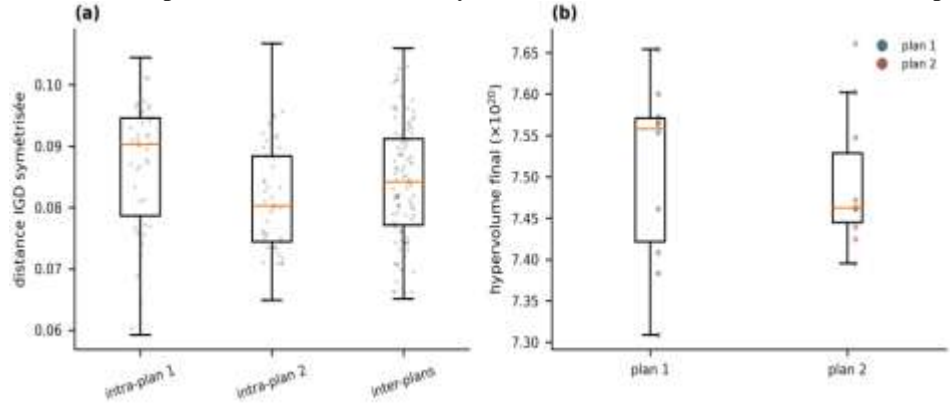

Figure 11. Dispersion between searches.

Figure 11 assesses the stability of the performance obtained when the search is repeated. Panel (a) compares the dispersion among searches using the same plan to that observed between the two sampling plans. Panel (b) compares the final hypervolume distributions. The small difference between these distributions indicates that the chosen energy, thermal, and economic trade-offs are not related to a single initial draw.11 11

Figure 12 shows the distribution of mixed comfort, thermal resilience and their relationship with annual energy.

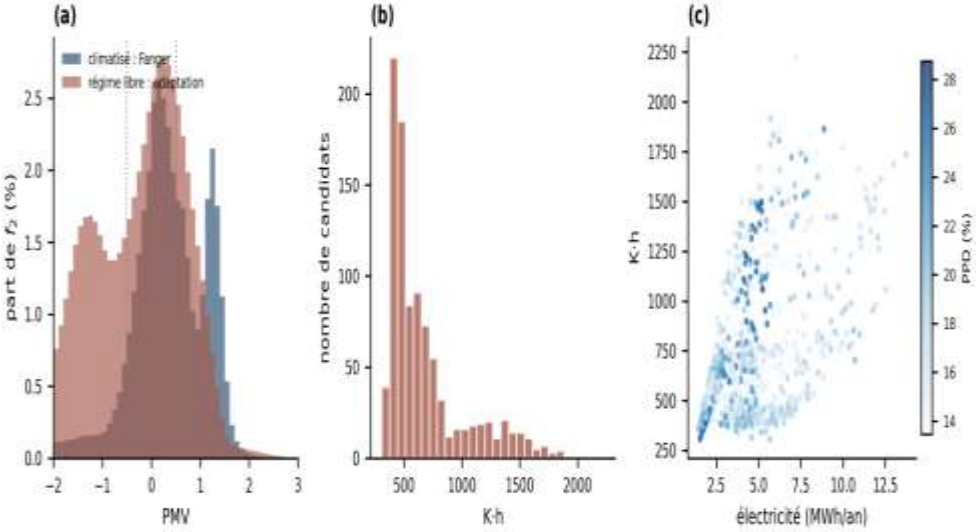

Figure 12. Comfort and resilience.

Figure 12 completes the analysis of the building's thermal performance. Figure 12a distinguishes the contributions to comfort depending on whether the air conditioning is active or not. Figure 12b shows the distribution of degree-hours of overheating when air conditioning is unavailable. Figure 12c relates annual electricity consumption to thermal resilience and discomfort. These three aspects must be considered together: a low-consumption configuration during normal operation is not necessarily the one that maintains the most stable thermal conditions during a power outage.

Recommendations extracted from the Pareto principle:-

Two criteria extract a recommendation from the final validated compromise. The no-regrets compromise minimizes the distance to an ideal where each of the five objectives would be at its minimum, after normalization on the final Pareto front and with equal weights. For each of the five objectives , we setj

$$z_j(x)=\frac{f_j(x)-f_j^{min}}{f_j^{max}-f_j^{min}},\ d_{SR}(x)=\left(\frac{1}{5}\sum_{j=1}^{5} z_j(x)^2\right)^{1/2}, \quad (18)$$

And the no-regret recommendation is the candidate P_{412} who minimizes costs d_{SR}. The lowest cost minimizes the total expense over twenty years, including construction, maintenance, replacements, and electricity bills.

$$C_{20}(x)=f_3(x)+C_{elec,20}(x). \quad (19)$$

Both recommendations belong to the final validated Pareto front of 412 building configurations.

The two approaches converge on three choices: compacted laterite walls, palm kernel fiber insulation, and minimal roof overhang. They diverge on the fan configuration: the compromise approach involves installing fifteen fans at low speed; the cost-effective approach involves installing none, preferring to sacrifice comfort to save on the initial investment. This divergence illustrates the mechanics of ventilation: its comfort cost decreases with the chosen speed but never reaches zero; a criterion that considers only cost ultimately leads to a preference for doing without it.

Laterite was chosen not for its poor thermal resistance, but for its thermal inertia: it dampens the peak load, thus reducing the required air conditioning capacity without decreasing annual energy consumption. The highly reflective roof limits direct solar gain, which is dominant in lower latitudes; painting the roof a light color costs several thousand francs, whereas further insulation provides only diminishing returns.

Discussion:-

The results of this study can be compared to three sets of research: studies on the coupling of ceiling fans and air conditioning, thermal comfort studies conducted in hot climates, and multi-objective building optimization approaches. However, the comparison must take into account differences in building typology, climate, systems studied, and indicators used. Table 11 summarizes the positioning of this study in relation to the most directly applicable works among the references already cited.

Table 11. Comparative positioning of the present study in relation to selected previous works

Study	Scope and approach	Relevance to the present study
Schiavon and Melikov [4]	Effects of increased air movement on energy savings and comfort.	Confirms the benefit of air movement, but does not by itself cover the joint optimization of the building envelope, equipment and their own consumption.
Raftery et al. [5]	Two-year evaluation of automated ceiling fans operating in coordination with air conditioning.	This provides a direct point of comparison for combined fan-air conditioning operation. The present study extends the analysis to the building design and accounts for the electricity and heat dissipated by the fans.
Kent et al. [6]	Energy savings and thermal comfort in a net-zero energy office building equipped with fans, in Singapore.	This study provides evidence on fan performance in tropical climates. However, this particular study focuses on a single-family dwelling and seeks a compromise between five objectives.
Kiki et al. [8]; Ogbonna and Harris [9]; Nematchoua et al. [12]	Field studies on thermal comfort in buildings located in hot or tropical climates of Africa.	This research highlights the importance of the climatic context and local thermal responses. It justifies the need to avoid indiscriminately applying comfort thresholds established in different climates.
Nguyen et al. [18]; Cruz et al. [19]; Stevanović et al. [30]	Review of simulation optimization methods, review of surrogate models for sustainable design and comparison of predictive models.	This work situates the use of surrogate models in building optimization. The present study adds a final verification of the solutions through full EnergyPlus simulations and repeats the research on twenty initializations.

Study	Scope and approach	Relevance to the present study
Bibang Bi Obam Assoumou et al. [21]; Bokhari and Ali [22]	Passive optimization of building envelopes in tropical climates and energy/carbon optimization of residential buildings in hot climates.	These studies provide points of comparison for optimizing the building envelope and achieving energy and carbon targets. This study links these dimensions to comfort, cost, and resilience in the event of a power outage.

Studies on air movement show that fans can improve comfort and help reduce the need for air conditioning [4–6]. This study confirms the value of this strategy but specifies the necessary condition for its evaluation: the fan must be treated as an electrically consuming device whose heat is also released into the area. In the 5,994 configurations simulated, fans accounted for a median of 16.9% of the total electricity consumption, with values reaching as high as 83.3%. Their contribution cannot therefore be considered negligible. An analysis limited to the reduction in compressor consumption would risk overestimating the net gain from air movement, particularly when the number of units increases. The energy efficiency of the fan thus depends on the increase in the air conditioning setpoint it enables, as well as its electrical power and control method.

This reading complements the experimental and simulation results of Schiavon and Melikov [4], Raftery et al. [5], and Kent et al. [6]. These works establish the relevance of air movement and the coordinated operation of fans and air conditioning. The main difference lies in the scope of the evaluation: here, air movement is not studied in isolation or within a fixed envelope. The number of ceiling fans, their speed, activation thresholds, natural ventilation, glazing, walls, and roof insulation are optimized within the same design space. The result, therefore, does not constitute a direct replication of the savings reported in these studies, but rather a broader analysis of the trade-offs between total energy consumption, discomfort, and building characteristics.

The issue of comfort must also be interpreted in light of field studies conducted in West Africa and other tropical regions [8–13]. These studies show that comfort assessment depends on the climate, the type of building, and the occupants' ability to adapt. Adaptive models and studies on the limitations of PMV in naturally ventilated environments [14–17, 36, 40] reinforce the need to distinguish between periods with air conditioning and periods with natural ventilation or air movement. In the present study, comfort is calculated hour by hour according to the actually simulated regime, and the cooling effect associated with air velocity is taken into account in accordance with the method adopted in ASHRAE 55 [41]. This formulation avoids applying the same treatment uniformly to periods with and without air conditioning. However, it does not replace a comfort survey of the occupants of the studied dwelling; the results remain those of a numerical assessment.

In terms of the building envelope, optimization studies in tropical or hot climates [21, 22] confirm the value of jointly examining construction choices and energy performance. This study extends this approach by considering five objectives: annual electricity consumption, discomfort, discounted cost, embodied carbon, and overheating during power outages. The results show that economic and environmental choices do not necessarily lead to the same material. Compacted laterite is at the more economical end of the spectrum, while adobe achieves the lowest embodied carbon values in the catalog studied. The fact that no concrete or cement-stabilized compressed earth block (CEB) walls appear among the 445 candidates retained after overall validation is a result specific to the building, the variable ranges, and the assumptions regarding cost, lifespan, and emissions. It does not allow us to conclude that raw earth is universally superior.

The stability of this result was examined by perturbing the catalog prices and emission factors by ±20%. The distribution between adobe and laterite then varies by a few tenths of a point, while concrete remains absent from the selected configurations. This robustness applies to the tested perturbations; it does not eliminate the uncertainty related to local cost, maintenance, and lifespan data. In particular, the maintenance costs of earthen walls are catalog assumptions and not observations from long-term monitoring in Benin. The economic comparison with a concrete block construction should therefore be interpreted as a comparison conditional on the assumptions made, and not as a cost guarantee for any project.

The computational approach builds on previous work on building optimization through simulation and on surrogate models [18, 19, 26, 27, 30]. Its advantage lies in reducing the number of costly evaluations while maintaining physical verification of the selected solutions. The twenty independent searches generated 5,994 simulated configurations; the 972 configurations selected from the final fronts were then re-evaluated in EnergyPlus. The mean relative prediction error is no greater than 4.29% for each of the five objectives. After comparison with the overall

database, 445 candidates are not dominated by any of the simulated configurations, and 412 constitute the final front after the second dominance analysis. This procedure provides a more robust level of verification than a selection based solely on metamodel predictions. However, it does not prove that the overall mathematical minimum has been reached: the resulting front remains dependent on the computational budget, the design domains, and the physical models.

Several limitations must be considered before any extrapolation of the results. First, temperature and air velocity are assumed to be uniform in each zone, whereas the velocity field created by a ceiling fan is spatially heterogeneous [31]. The calculated comfort therefore represents an approximation at the zone scale and not a local map of occupant exposure. Second, the volume-weighted average infiltration rate of 0.278 h^{-1} is based on an assumption from the literature and was not measured by blower door testing in a comparable Beninese dwelling. Third, air exchange between adjacent zones is not explicitly modeled due to the lack of measured leakage coefficients. Finally, the distribution factor associated with natural ventilation is based on the order of magnitude attributed to Givoni [62], whose primary source could not be identified in this study. These assumptions can affect the absolute values of comfort and ventilation, even though sensitivity analyses indicate that infiltration parameters do not directly drive the material composition of the Pareto front.

Future work will therefore need to compare the model with in-situ measurements of temperature, humidity, air velocity, and electricity consumption, as well as with an airtightness measurement campaign. A spatial characterization of air movement under the fan would also allow for a better correlation between simulated velocities and actual perceived comfort. Finally, it would be useful to extend the optimization to multiple dwellings, other West African climates, and local material catalogs that better document maintenance costs, lifespans, and embodied carbon. These validations would allow us to distinguish regulatory mechanisms that could be generalized from material choices that remain dependent on the local economic and construction context.

Conclusion :-

The main practical implications of the results are as follows:-

- The fan activation threshold should be calibrated first: this variable accounts for 42.7% of the variation in annual energy use and entails no additional capital cost.
- A clear trade-off must be made between the number of ceiling fans and the cost, as optimal compromise solutions install fifteen low-speed fans at the low-speed setting. The most cost-effective building configuration installs none. The right choice depends on the decision-maker's priorities, not on a single rule.
- Earthen wall materials should be considered, with the choice between compacted laterite and adobe depending on the relative importance assigned to cost and embodied carbon. None of the 972 verified configurations uses concrete or cement-stabilized earth blocks.
- Use a high-reflectance roof finish before insulating further because high reflectance costs a few thousand francs and eliminates a major source of solar heat gains for a low building in low latitudes.
- Never publish a Pareto front obtained from a single stochastic search without comparing it to a second one because the difference between the two initial sampling plans of this study remains less than the dispersion between searches of the same sample: it is this observation, and not an intuition, which allows the material composition of the Pareto front to be published as a result rather than as a seed artifact.

Including the heat and electricity consumption of the ceiling fan changes the answer: the fan, often considered negligible, accounts for 16.9% of the total electricity consumption at the median. Twenty independent studies, totaling 5994 simulated configurations, confirm a result that a single study could not have established with the same certainty: no concrete or conventional block walls appear among the 445 candidates retained after validation; only the two raw-earth wall options are represented.

Conflicts of interest:-

The authors declare that they have no known competing financial interests or personal relationships that could have appeared to influence the work reported in this paper.

Contributions des auteurs:-

BOME Brice :

Conceptualization, Methodology, Software, Investigation, Formal analysis, Data curation, Visualization, Writing – original draft.

Fannou Jean-Louis Comlan:-
Methodology, Validation, Supervision, Writing – review & editing.

Tokpohozin Noukpo Bernard:-
Methodology, Validation, Writing – review & editing.

HOUNGAN Comlan Aristide:-
Supervision, Project administration, Writing – review & editing. All authors have read and approved the final version of the manuscript.

References:-

1. Falchetta, G., Mistry, M. (2021). The role of residential air movement and cooling demand for electrification planning: Implications of climate change in sub-Saharan Africa. Energy Economics 99, 105307. doi:10.1016/j.eneco.2021.105307
2. Sailor, D. (2003). Air conditioning market saturation and long-term response of residential cooling energy demand to climate change. Energy 28(9), 941–951. doi:10.1016/s0360-5442(03)00033-1
3. Dodoo, Ambrose and Ayarkwa, Joshua (2019). Effects of climate change for thermal comfort and energy performance of residential buildings in a sub-Saharan African climate. Buildings 9(10), 215. doi:10.3390/buildings9100215.
4. Schiavon, S., Melikov, A. (2008). Energy saving and improved comfort by increased air movement. Energy and Buildings 40(10), 1954–1960. doi:10.1016/j.enbuild.2008.05.001
5. Raftery, P., Douglass-Jaimes, D., Sanguinetti, A. et al. (2022). Cooling energy savings and occupant feedback in a two year retrofit evaluation of 99 automated ceiling fans staged with air conditioning. Energy and Buildings 254, 111189. doi:10.1016/j.enbuild.2021.111189
6. Kent, Michael G. and Huynh, Nam Khoa and Mishra, Asit Kumar and Tartarini, Federico and Lipczynska, Aleksandra and Li, Jiayu and Sultan, Zurami and Goh, Edwin and Karunagaran, Giridharan and Natarajan, Arulmani and Indrajith, Asiri and Hendri, Ivanna and Narendra, Komang I. and Wu, Vicky and Chin, Noel and Gao, Chun Ping and Sapar, Majid and Seoh, Alvin and Shuhadah, Nur and Valliappan, Selvam and Jukes, Tim and Spanos, Costas and Schiavon, Stefano (2023). Energy savings and thermal comfort in a zero energy office building with fans in Singapore. Building and Environment 243, 110674. doi:10.1016/j.buildenv.2023.110674.
7. Center for the Built Environment (2024). Ceiling Fan Design Guide : Elevated air speed and thermal comfort. CBE Berkeley, online guide.
8. Kiki, G., Kouchadé, C., Houngan, A., Zannou-Tchoko, S. et al. (2020). Evaluation of thermal comfort in an office building in the humid tropical climate of Benin. Building and Environment 185, 107277. doi:10.1016/j.buildenv.2020.107277
9. Ogbonna, A. C., Harris, D. J. (2008). Thermal comfort in sub-Saharan Africa: Field study report in Jos-Nigeria. Applied Energy 85(1), 1–11. doi:10.1016/j.apenergy.2007.06.005
10. Mohammadpourkarbasi, Haniyeh and Jackson, Iain and Nukpezah, Daniel and Appeaning Addo, Irene and Assasie Oppong, Rexford (2022). Evaluation of thermal comfort in library buildings in the tropical climate of Kumasi, Ghana. Energy and Buildings 268, 112210. doi:10.1016/j.enbuild.2022.112210.
11. Yadeta, Chali and Indraganti, Madhavi and Terefe Tucho, Gudina and Alemayehu, Esayas (2023). Study on adaptive thermal comfort model and behavioral adaptation in naturally ventilated residential buildings, Jimma Town, Ethiopia. Energy and Buildings 298, 113483. doi:10.1016/j.enbuild.2023.113483.
12. Nematchoua, Modeste Kameni and Tchinda, René and Ricciardi, Paola and Djongyang, Noël (2014). A field study on thermal comfort in naturally-ventilated buildings located in the equatorial climatic region of Cameroon. Renewable and Sustainable Energy Reviews 39, 381–393. doi:10.1016/j.rser.2014.07.010.
13. Munonye, Charles and Ji, Yingchun (2020). Evaluating the perception of thermal environment in naturally ventilated schools in a warm and humid climate in Nigeria. Building Services Engineering Research and Technology 42(1), 5–25. doi:10.1177/0143624420911148.
14. Nicol, J.F. and Humphreys, M.A. (2002). Adaptive thermal comfort and sustainable thermal standards for buildings. Energy and Buildings 34(6), 563–572. doi:10.1016/S0378-7788(02)00006-3.
15. Humphreys, Michael A and Fergus Nicol, J (2002). The validity of ISO-PMV for predicting comfort votes in every-day thermal environments. Energy and Buildings 34(6), 667–684. doi:10.1016/S0378-7788(02)00018-X.
16. Ze Ze, Cyrille Brice and Nneme Nneme, Léandre and Monkam, Louis (2024). PMVd/PPDd model for predicting thermal comfort in air-conditioned buildings in hot and humid regions of Sub-Saharan Africa. International Journal of Air-Conditioning and Refrigeration 32(1). doi:10.1007/s44189-024-00061-z.

17. Yao, Runming and Li, Baizhan and Liu, Jing (2009). A theoretical adaptive model of thermal comfort : Adaptive Predicted Mean Vote (aPMV). Building and Environment 44(10), 2089–2096. doi:10.1016/j.buildenv.2009.02.014.
18. Nguyen, Anh-Tuan and Reiter, Sigrid and Rigo, Philippe (2014). A review on simulation-based optimization methods applied to building performance analysis. Applied Energy 113, 1043–1058. doi:10.1016/j.apenergy.2013.08.061.
19. Cruz, A. S. and Caldas, L. R. and Mendes, V. M. and Mendes, J. C. and Bastos, L. E. G. (2024). Multi-objective optimization based on surrogate models for sustainable building design: A systematic literature review. Building and Environment 266, 112147. doi:10.1016/j.buildenv.2024.112147.
20. Li, Rong and Shari, Zalina and Ab Kadir, Mohd Zainal Abidin (2024). A review on multi-objective optimization of building performance : Insights from bibliometric analysis. doi:10.2139/ssrn.4889780.
21. Bibang Bi Obam Assoumou, Stahel Serano and Zhu, Li and Elenga, Rolains Golchimard (2026). Multiobjective passive optimization of building envelopes integrated phase change material in tropical climate: a case of Gabon. Journal of Engineering Research 14(2), 1221–1231. doi:10.1016/j.jer.2025.12.020.
22. Bokhari, Ali and Ali, Khuloud (2026). Simulation-based evolutionary optimization of residential buildings for energy and carbon reduction across warm–humid and coastal hot–arid climates. Buildings 16(11), 2157. doi:10.3390/buildings16112157.
23. Deb, K. and Pratap, A. and Agarwal, S. and Meyarivan, T. (2002). A fast and elitist multiobjective genetic algorithm: NSGA-II. IEEE Transactions on Evolutionary Computation 6(2), 182–197. doi:10.1109/4235.996017.
24. Deb, K., Jain, H. (2014). An Evolutionary Many-Objective Optimization Algorithm Using Reference-Point-Based Nondominated Sorting Approach, Part I: Solving Problems With Box Constraints. IEEE Transactions on Evolutionary Computation 18(4), 577–601. doi:10.1109/TEVC.2013.2281535
25. Laumanns, M., Thiele, L., Deb, K., Zitzler, E. (2002). Combining convergence and diversity in evolutionary multiobjective optimization. Evolutionary Computation 10(3), 263–282. doi:10.1162/106365602760234108
26. Forrester, Alexander I.J. and Keane, Andy J. (2009). Recent advances in surrogate-based optimization. Progress in Aerospace Sciences 45(1-3), 50–79. doi:10.1016/j.paerosci.2008.11.001.
27. Jones, Donald R. and Schonlau, Matthias and Welch, William J. (1998). Efficient global optimization of expensive black-box functions. Journal of Global Optimization 13(4), 455–492. doi:10.1023/A:1008306431147.
28. Grinsztajn, Léo and Oyallon, Edouard and Varoquaux, Gaël (2022). Why do tree-based models still outperform deep learning on typical tabular data?. In Advances in Neural Information Processing Systems 35 (NeurIPS 2022), Datasets and Benchmarks Track.
29. Shwartz-Ziv, Ravid and Armon, Amitai (2022). Tabular data: Deep learning is not all you need. Information Fusion 81, 84–90. doi:10.1016/j.inffus.2021.11.011.
30. Stevanović, Sanja and Dashti, Hesam and Milošević, Miloš and Al-Yakoob, Salem and Stevanović, Dragan (2024). Comparison of ANN and XGBoost surrogate models trained on small numbers of building energy simulations. PLoS ONE 19(10), e0312573. doi:10.1371/journal.pone.0312573.
31. Raftery, P., Fizer, J., Chen, W., He, Y. et al. (2019). Ceiling fans: Predicting indoor air speeds based on full scale laboratory measurements. Building and Environment 155, 210–223. doi:10.1016/j.buildenv.2019.03.040
32. Crawley, D. B., Lawrie, L. K., Winkelmann, F. C. et al. (2001). EnergyPlus: creating a new-generation building energy simulation program. Energy and Buildings 33(4), 319–331. doi:10.1016/S0378-7788(00)00114-6
33. U.S. Department of Energy (2025). EnergyPlus Version 25.2.0 Engineering Reference. DOE Building Technologies Office.
34. [34] Lawrie, L. K., Crawley, D. B. (2026). Development of Global Typical Meteorological Years (TMYx). https://climate.onebuilding.org. File used: BEN_ZO_Bohicon.653380_TMYx.epw.https://climate.onebuilding.org
35. Stull, R. (2011). Wet-bulb temperature from relative humidity and air temperature. Journal of Applied Meteorology and Climatology 50(11), 2267–2269. doi:10.1175/JAMC-D-11-0143.1
36. de Dear, R. J., Brager, G. S. (2002). Thermal comfort in naturally ventilated buildings: revisions to ASHRAE Standard 55. Energy and Buildings 34(6), 549–561. doi:10.1016/S0378-7788(02)00005-1
37. CEN (2019). EN 16798-1:2019 : Energy performance of buildings: Ventilation for buildings. European Committee for Standardization.
38. ISO (2005). ISO 7730:2005, Ergonomics of thermal environments: analytical determination and interpretation of thermal comfort by calculation of PMV and PPD indices and by local thermal comfort criteria . International Organization for Standardization , Geneva.
39. International Organization for Standardization (2021). ISO 8996:2021: Ergonomics of the thermal environment: Determination of metabolic rate . ISO, Geneva.

40. Fanger, P.O., Toftum, J. (2002). Extension of the PMV model to non-air-conditioned buildings in warm climates. Energy and Buildings 34(6), 533–536. doi:10.1016/S0378-7788(02)00003-8
41. ANSI/ASHRAE (2023). Standard 55-2023, Thermal Environmental Conditions for Human Occupancy. ASHRAE, Atlanta, §5.3.3.1 and Appendix C (Cooling Effect method, based on Gagge's two-node model).
42. ASHRAE (2013). ANSI/ASHRAE Standard 55-2013: Thermal Environmental Conditions for Human Occupancy. American Society of Heating, Refrigerating and Air-Conditioning Engineers, Atlanta.
43. ASHRAE (2020). ANSI/ASHRAE Standard 55-2020: Thermal Environmental Conditions for Human Occupancy. ASHRAE, Atlanta.
44. Gagge, A. P., Fobelets, A. P., Berglund, L. G. (1986). A standard predictive index of human response to the thermal environment. ASHRAE Transactions 92, 709–731.
45. CEN (2022). EN 14825:2022 : Air conditioners, liquid chilling packages and heat pumps: Testing and rating at part load conditions. CEN.
46. ASHRAE (2017). 2017 ASHRAE Handbook : Fundamentals, Chapter 16: Ventilation and Infiltration. ASHRAE, Atlanta. ISBN 978-1-939200-57-0.
47. Air Conditioning Contractors of America (2023). ANSI/ACCA 3 Manual S : Residential Equipment Selection. ACCA.
48. CYPE (2024). CYPE 2024: Catalogue general. CYPE, catalogue documentaire 2024.
49. ISO (2007). ISO 10456:2007 : Building materials and products: Hygrothermal properties, tabulated design values and procedures for determining declared and design thermal values. International Organization for Standardization, Geneva.
50. Muthuraj, Rajendran and Lacoste, Clément and Lacroix, Patrick and Bergeret, Anne (2019). Sustainable thermal insulation biocomposites from rice husk, wheat husk, wood fibers and textile waste fibers: elaboration and performances evaluation. Industrial Crops and Products 135, 238–245. doi:10.1016/j.indcrop.2019.04.053.
51. Brockhoff, D., Zitzler, E. (2006). Are all objectives necessary? On dimensionality reduction in evolutionary multiobjective optimization. In Parallel Problem Solving from Nature (PPSN IX), LNCS 4193, 533–542. doi:10.1007/11844297_54
52. IPCC (2021). Climate Change 2021: The Physical Science Basis. Chapter 7, Appendix 7.A : Global Warming Potentials. Cambridge University Press.
53. Chartered Institution of Building Services Engineers (2021). TM65: Embodied carbon in building services : a calculation methodology. CIBSE.
54. Das, I., Dennis, J. E. (1998). Normal-boundary intersection: a new method for generating the Pareto surface in nonlinear multicriteria optimization problems. SIAM Journal on Optimization 8(3), 631–657. doi:10.1137/S1052623496307510
55. Sobol', I.M (1967). On the distribution of points in a cube and the approximate evaluation of integrals. USSR Computational Mathematics and Mathematical Physics 7(4), 86–112. doi:10.1016/0041-5553(67)90144-9.
56. Owen, A. B. (1998). Scrambling Sobol' and Niederreiter–Xing points. Journal of Complexity 14(4), 466–489. doi:10.1006/jcom.1998.0487
57. McKay, M. D. and Beckman, R. J. and Conover, W. J. (1979). Comparison of Three Methods for Selecting Values of Input Variables in the Analysis of Output from a Computer Code. Technometrics 21(2), 239–245. doi:10.1080/00401706.1979.10489755.
58. Zitzler, Eckart and Thiele, Lothar (1999). Multiobjective evolutionary algorithms: A comparative case study and the strength Pareto approach. IEEE Transactions on Evolutionary Computation 3(4), 257–271. doi:10.1109/4235.797969.
59. Owen, Art B. (2014). Sobol' indices and Shapley value. SIAM/ASA Journal on Uncertainty Quantification 2(1), 245–251. doi:10.1137/130936233.
60. Song, Eunhye and Nelson, Barry L. and Staum, Jeremy (2016). Shapley effects for global sensitivity analysis: Theory and computation. SIAM/ASA Journal on Uncertainty Quantification 4(1), 1060–1083. doi:10.1137/15M1048070.
61. Iooss, Bertrand and Prieur, Clémentine (2019). Shapley effects for sensitivity analysis with correlated inputs: comparisons with Sobol' indices, numerical estimation and applications. International Journal for Uncertainty Quantification 9(5), 493–514. doi:10.1615/Int.J.UncertaintyQuantification.2019028372.
62. Givoni, B. (1992). Comfort, climate analysis and building design guidelines. Energy and Buildings 18(1), 11–23. doi:10.1016/0378-7788(92)90047-K.
63. Wong, Bang (2011). Points of view: Color blindness. Nature Methods 8(6), 441–441. doi:10.1038/nmeth.1618.